Basics and Applications of Electrowetting on Dielectric (EW)

Dineshkumar Y. Turkar, Sandip M. Wadhai, Yogesh B. Sawane and Arun G. Banpurkar*

Department of Physics,
S P Pune University, Pune-411007
*e-mail: agb@physics.unipune.ac.in

(Submitted: 31-12-2014)

Abstract

The shape of liquid-droplet on planar surfaces is mainly governed by resultant surface tension forces at the vapour-liquid-solid boundary. In thermodynamic equilibrium, wetting of liquid or contact angle (CA) is given by Young-Dupr'e equation which is related to surface tensions of liquid, solid and interfacial tension of liquid-solid. The irreversible change in equilibrium wetting is possible by altering the surfaces and/or adding surfactant in the liquid. However, controlled and reversible wetting is desired in several applications like liquid-lens, ink-jet printing, droplet transport through micro-fluidic chip etc. Currently this is achieved by incident light, electric field, thermal gradient, magnetic field etc. The electric field induced wetting commonly termed as Electrowetting on dielectric (EWOD or EW) is the most successful method allowing fast and reversible change in wetting of aqueous and non aqueous droplet on dielectric surfaces. EW is currently implemented in variety of applications such as video displays, adaptive lens systems in cell-phone cameras, smart window panels etc. In the present review, we discuss basic EW phenomenon and governing equations. The experimental results related to EW based liquid lens system are discussed. The upcoming technology and challenges of EW are discussed at the end.

Introduction:

The dew on a grass leaves and spider web appears as if pearl necklaces fascinating the mankind since long time. The water bead on "Lotus" leaf has been a symbol of eternal purity from all the odds… "*One who does all work as an offering to the Lord, abandoning attachment to the results, is as untouched by sin [or Karmic reaction] as a lotus leaf is untouched by water (Bhaqaved Gita).* New born baby starts her effortless breath due to presence of surfactant in the alveoli. Trouble free washing of utensil and cloths take place in presence of magic liquid called detergent, oil recovery from reservoir requires additives in the water.…there is endless list of applications that requires basic understanding of wetting property of liquid on solid surfaces and their control.

Thomas Young in 1805 has described the equilibrium wetting of liquid droplet on plane surface in terms of contact angle made by the liquid on solid surface[1]. This mathematical equation is based on the force balance at the air-liquid-solid interface called as three-phase contact line (TCL). Figure 1 illustrates this force balance at TCL.

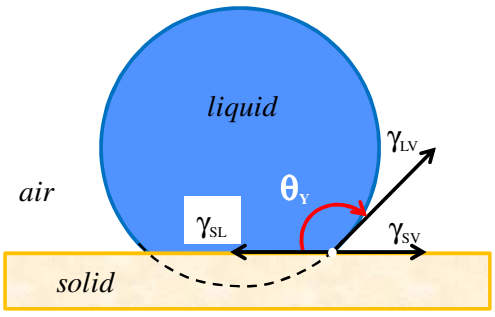

Fig. 1: The contact angle θ_Y on a planar surface is due to surface tension force balanced at every point of TCL

Young-Dupr'e equation relating surface tensions to the contact angle is given as

$$cos\theta_Y = \frac{\gamma_{SV}-\gamma_{SL}}{\gamma_{LV}} \quad \ldots\ldots\ldots\ldots\ldots\ldots\ldots\ldots\ldots\ldots(1)$$

Where θ_Y is Young's contact angle and surface tension forces described as γ_{SL} – solid-liquid, γ_{SV} –solid-vapour and γ_{LV} – liquid-vapour. This clearly shows that the contact angle of liquid is mainly related to surface tensions.

Many times surface-tension force can also be viewed as surface energy per unit area therefore above Young's condition could be obtained by minimizing surface-energy for constant droplet volume. Thus free liquid volume forms spherical shape to minimize surface energy. The gravitational force also influences the shape of liquid volume. The interplay of the gravity and surface tension forces allows the liquid to form a bead or puddle. This is decided by the parameter called capillary length, $\boldsymbol{\kappa^{-1}} = \sqrt{\boldsymbol{\gamma/\rho g}}$ where $\boldsymbol{\rho g}$ is gravitational force per unit volume and γ is liquid surface energy per unit area. For instance capillary length for water is 2.73 mm, hence water droplet below 2.7 mm size favour spherical shape while above this size, it forms a puddle.

Many planar surfaces like polymer sheets, metals and metal-oxides coated surfaces exhibits varied contact angle for water. On the basis of water

contact angle (θ_Y) surfaces are characterized as hydrophilic surface ($0° < \theta_Y < 90°$), hydrophobic surface ($90° \leq \theta_Y < 150°$) and superhydrophobic surface ($150° \leq \theta_Y < 180°$). Thus Lotus leaf and many plant surfaces exhibit superhydrophobic state. And complete spreading of water on clean glass shows hydrophilic state of glass.

In addition to the naïve definitions of the wetting, Zisman showed that the wettability of a liquid on surfaces is not only decided by the surface energy of solids or liquids but it depends on the polarizibilities[2]. Zisman's rule says that 'A liquid spreads completely if it is less ploarizable than the solid' which in general explains why liquid Helium with its low polarizibility spreads on most solid. Also spreading of oil on water surface is due high polarizability of water than oils. Therefore changing polarizibility at liquid-solid interface is necessary for alteration in wetting.

Several conventional techniques are currently used to bring changes in wetting on solid surfaces. For instance, thermal gradient at interface changes surface tensions of both liquid and solids is termed as thermo-capillarity[3]. In the photowetting, the light on solid-liquid interface is made incident to alter the surface tensions hence changes CA [4]. In case of magneto-wettting, external magnetic field is used to induce the wetting. Also external electric field is used to alter this wetting is known as electrowetting[5]. Out of these above schemes Electrowetting has gain tremendous impetus due to several advantages in design and simplicity of the process. This is also commonly called as electrowetting on dielectric (EWOD) or electrowetting (EW). This technique is very successful in changing surface-energy or contact angle of liquid on dielectric surface by several degrees ($\Delta\theta \sim 70$ to 90^o) with the application of electric voltage across the droplet and the control electrode buried in the dielectric.

Figure 2 shows generic EW setup used to change the wetting of conductive liquid on dielectric surface.

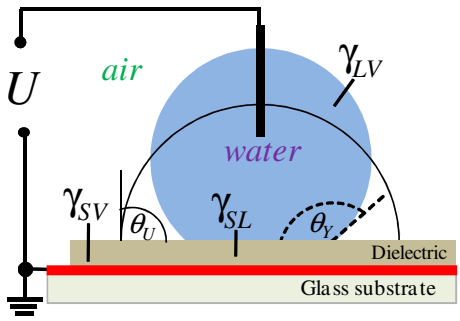

Fig. 2: Schematic shows basic EW setup the conductive electrode buried in the dielectric is shown in red colour.

Here U is an external voltage either low frequency alternating current (AC) or direct current (DC). The Young's contact angle is denoted by θ_Y at U = 0 V and reduction in CA for external voltage U is shown by $\theta(U)$. Another wire free geometry is most common wherein electric field is applied between electrodes buried in the dielectric as shown in Fig 3 and liquid droplet is free from any direct electrical contacts.

In both these cases electrical charge density or polarization at the liquid-solid interfaces is altered by the external applied voltage. Thus evolution of electrostatic energy at solid-liquid interface due to electric charge density alters surface-energy balance at solid-liquid interface changing the wetting of liquid as function of external voltage. The electrostatic energy due to charge density reduces to zero upon removal of the external voltage restoring normal wetting state of the liquid. Therefore, EW process is fast and can be realized on the time scale of the droplet hydrodynamic relaxation time scales, which depends on viscosity, surface-tension and droplet size.

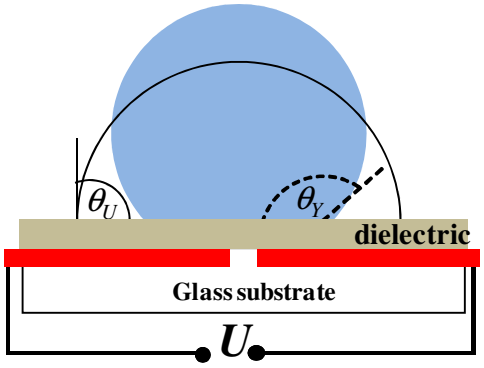

Fig. 3: Schematic shows wire-free EW setup and conductive electrodes (red) are buried in the dielectric.

The present form of the generic and wire–free electrowetting setups has been derived from the ingenious work on electro-capillarity by French Scientist Gabriel Lippmann's (1875)[6]. Lippmann showed that the height of the mercury in contact with diluted electrolyte in fine capillary tube is function of the voltage across the interface. An insulating double layer is often formed at two dissimilar electrolytes liquid interface analogous to the contact potential at metal-semiconductor junction. The electrical double-layer (EDL) at mercury-electrolyte interface is mainly due to the separations of ions at the interfaces. The EDL is feeble and break-down at moderate external voltage. Thus desired wetting is not possible on liquid-liquid interfaces. Lippmann electro-capillarity experiment was not attracted in past several years. After 1990 this phenomenon is revisited in new form. A thick dielectric layer is introduced at liquid-solid interface. A voltage is then applied between liquid and rigid planar electrode. Here dielectric layer avoids direct liquid contact with electrodes[7]. This is generic electrowetting geometry commonly known as electrowetting on dielectric (EWOD) or electrowetting (EW) which finds numerous application includes variable focal lenses[8], video speed display[9], laser mirrors and beam splitters[10], tensiometer[11], rheometers[12] and many digital (droplet) microfluidic devices for micro-fluidics and lab-on-chip devices[13].

In the present review, we used water drop of size about 1.5 mm which is blow capillary length hence surface tension dominates gravity force. Thus 1.5 mm size water droplet assumes near perfect spherical cap shape. At constant volume of droplet, the other geometrical parameters of spherical cap like base radius, radius of curvature etc. can be related to contact angle θ. Electrowetting is used to bring changes in contact angle θ using external voltage thus all geometrical parameters of spherical cap can be function of applied voltage.

After this brief introduction, we presented theoretical model for EW on spherical cap using Lippmann's approach. Subsequently energy minimization approach is presented to derive the same EW equation. The close form equations relating geometrical parameters of spherical cap as a function of contact angle is discussed. Basic experimental procedure for studying the EW is discussed in detail. Finally we present results and discussion on EW spherical cap as tunable liquid lens.

Electrowetting on Dielectric: EW equation shows variation in contact angle as function of voltage magnitude. This is derived by Lippmann for the first time using thermodynamics and electro-chemical approach. In the following we present Lippmann's original approach and subsequently same relation is derived using energy minimization principle. Several other approaches for deriving EW equation can be found in review by J.C. Baret and F. Mugele[5]

(i)Thermodynamic and Electrochemical approach for EW equation:

Figure 4 shows generic EW setup with and without external voltage between conductive drop and bottom electrode. The presence of charges at interface due to external voltage between two conducting medium affects the surface tension of liquid drop in contact with dielectric, this is typically called as electrocapillarity[6]. Electric potential at the interface produces surface-charge density at the interface. We neglect the fringing field at the droplet boundary and try to setup an equation of the thermodynamic energy change.

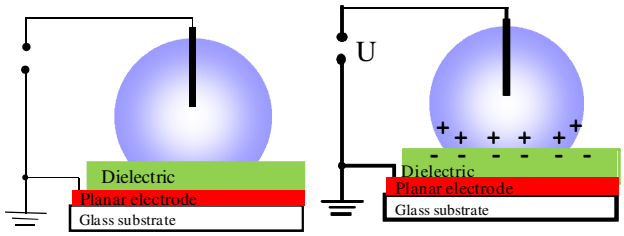

Fig. 4 Schematic shows generic setup and change density at the liquid-solid interface.

At equilibrium temperature T and pressure P, The thermodynamic potential (Gibbs free energy) is given by[14]

$$dG = \gamma\, dA - edU \quad \ldots\ldots\ldots\ldots\ldots\ldots\ldots\ldots\ldots\ldots(2)$$

Where γ is surface tension and e is electronic charge at interface. dG is change in thermodynamic free energy for external voltage dU. Here γdA is the work done in reversible change dA in area A of the surface of separation.

Thermodynamic potential is replaced by its surface part only at constant pressure and temperature.

$$dG_s = \gamma_{SL} dA - edU \quad \ldots\ldots\ldots\ldots\ldots\ldots\ldots\ldots\ldots\ldots(3)$$

At constant potential U, dU = 0 and above eq. becomes

$$G_s = \gamma_{SL} A \quad \ldots\ldots\ldots\ldots\ldots\ldots\ldots\ldots\ldots\ldots\ldots\ldots(4)$$

Upon applying voltage dU an electric charge density builds up spontaneously at solid-liquid interface consisting of charge on metal surface other oppositely charged ions on liquid side interface. It results in reduction of surface tension as:

$$d\gamma_{eff} = -\sigma_{SL} dU \quad \ldots\ldots\ldots\ldots\ldots\ldots\ldots\ldots\ldots\ldots(5)$$

Where, σ_{sl} is surface charge density at solid-liquid interface. Total effective surface tension between solid liquid is obtained by integrating above Eq. 5

$$\gamma_{SL}^{eff} = \gamma_{SL} - \int_0^U \sigma_{SL} dU \quad \ldots\ldots\ldots\ldots\ldots\ldots\ldots\ldots\ldots\ldots(6)$$

$$\gamma_{SL}^{eff} = \gamma_{SL} - \frac{C^* U^2}{2} \quad \ldots\ldots\ldots\ldots\ldots\ldots\ldots\ldots\ldots\ldots(7)$$

Where capacitance per unit area, $C^* = \frac{\varepsilon\varepsilon_0}{d}$ with $\varepsilon\varepsilon_0$ is permittivity and d is the thickness of the dielectric medium.

Young equation gives the equilibrium contact angle of liquid drop on solid surface is given by eq.1. Substituting the value of effective interfacial tension (Eq. 1) of solid in contact with liquid and in the presence of external voltage in Eq. 7, which reads as:

$$\cos\theta(U) = \cos\theta + \frac{C^* U^2}{2\gamma_{LV}} \text{ or}$$

$$\cos\theta(U) = \cos\theta + \frac{\varepsilon\varepsilon_O U^2}{2d\gamma_{LV}} \quad \ldots\ldots\ldots\ldots\ldots\ldots\ldots\ldots(8)$$

$$\cos\theta(U) = \cos\theta + \eta \quad \ldots\ldots\ldots\ldots\ldots\ldots\ldots\ldots\ldots\ldots(9)$$

where $\eta = \frac{\varepsilon\varepsilon_O U^2}{2d\gamma_{LV}}$ is the dimensionless electrowetting number indicates relative strength of electrical surface energy to interfacial surface energy. Equation 8 or 9 is termed as Young-Lippmann equation relating the change in contact angle with applied voltage U. This equation is valid for direct current (DC) and alternating

current (AC) voltages. In case of the AC voltage root mean square (r.m.s.) values are considered as voltage amplitude. The above equation is also derived using energy minimization.

(ii) EW Equation from Energy Minimization Approach[15]:

In this model total work done in setting charge density at liquid-solid interface and charge density withdrawn from the battery is considered. The energy from the battery is utilized to charge the liquid-solid interface and counter charge on the planar bottom electrodes as shown in Fig 5. The thermodynamics system is droplet, dielectric layer, metal electrode, and the voltage source (Battery). Throughout the derivation, we assume that the system is in equilibrium at constant potential *U* and at constant temperature *T*.

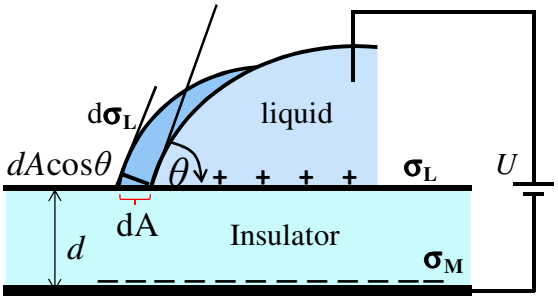

Fig. 5: A conductive droplet sitting on a dielectric surface. A battery perform work in setting a charge density at liqiod-solid interface and countercharge density at bottom conductive electode.

We focus on the change in free energy due to an infinitesimal increase in base area *dA* of the droplet on the solid surface surrounded by vapor. When a potential *U* is applied, a charge density σ_L is builds up in liquid phase and induces an image charge density σ_M on the metal electrode. An infinitesimal increase of the base area *dA* results in a contribution to the free energy from the surface energies also an energy contribution to the additional charge density $d\sigma_L$ liquid and its image charge density $d\sigma_M$ on the metal electrode. The voltage source performs work dW_B.

The free energy change (*dF*) of the system can be written as:

$$dF = \gamma_{SL}dA - \gamma_{SV}dA + \gamma_{LV}dA\cos\theta + dE_{el} - dW_B \quad \text{.....(10)}$$

where dE_{el} is energy stored in the electric field between the liquid and the counter electrode and dW_B is work done by the battery.

In the absence of external field $dE_{el} = dW_B = 0$ and on minimizing with respect to area $\frac{dF}{dA} = 0$ this gives Young Eq. (1)

For a non- zero potential, we need to include the energy of the charge distribution. We know that, the electrostatic energy per unit area below liquid is

$\frac{E_{el}}{A} = \int_0^d \frac{1}{2}\vec{E}\cdot\vec{D}\,dz$, where z is the coordinate perpendicular to the surface, *d* the thickness of the insulating layer, $\vec{E}$ the electric field, and $\vec{D}$ the charge displacement, with $\vec{D} = \varepsilon\varepsilon_0\vec{E}$.

The increase of free energy due to the charge distribution in the liquid, upon an infinitesimal increase of droplet base can be written as.

$\frac{dE_{el}}{dA} = \frac{U\sigma_L}{2}$. Where σ_L is the charge density at liquid-solid interface and *U* is electric voltage. The battery performs the work to redistribute the charges at interface as well as on the bottom electrode. Therefore the work done by the battery per unit area is given by $\frac{dW_B}{dA} = U\sigma_L$. Substituting these values in Eq. 10, we get

$$\frac{dF}{dA} = \gamma_{SL} - \gamma_{SV} + \gamma_{LV}\cos\theta + \frac{1}{2}U\sigma_L - U\sigma_L$$

At equilibrium, $\frac{dF}{dA}=0$, above equation becomes

$\gamma_{LV}\cos\theta(U)=\gamma_{SV}-\gamma_{SL}+\frac{1}{2}U\sigma_L$ which gives

$$\cos\theta(U)=\cos\theta+\frac{1}{2}\frac{U\sigma_L}{\gamma_{LV}}$$

now the charge density can be written as

$\sigma_L=E\varepsilon\varepsilon_0=\frac{U\varepsilon\varepsilon_0}{d}$ where $E=U/d$ is the electric field. Then above equation becomes

$$\cos\theta(U)=\cos\theta+\frac{1}{2}\frac{\varepsilon\varepsilon_0U^2}{d\,\gamma_{LV}}=\cos\theta+\eta \quad \ldots\ldots\ldots(11)$$

This is the same as Young's-Lippmann equation. The equation indicates that contact angle for a given voltage varies directly as permittivity of the dielectric medium and inversely with interfacial tension of the liquid. Thus a droplet of low interfacial tension on insulator of high dielectric constant is preferred in the EW. Equation 11 clearly indicates that with increasing voltage magnitude, the contact angle decreases and opposite is not possible. Thus high contact angle at zero voltage is desired for large tuning range. For instance, if the EW is performed on water droplet then low energy dielectric surface made from fluoropolymer with high dielectric breakdown field is preferred.

In most of the circumstances, oil ambient is used to reduce interfacial tension. Further it arrests the evaporation of aqueous droplet and provides thin lubricating film between droplet and substrate.

In the next section we present geometrical formalism for spherical cap of liquid drop.

Spherical Cap

A tiny liquid droplet sitting on the planar surface forms a spherical cap. It is a part of sphere as shown in Figure 6.

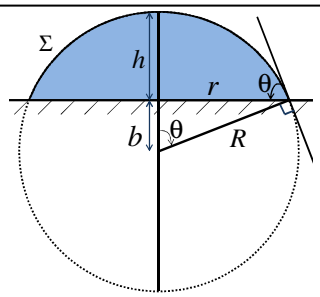

Fig. 6: A tiny water droplet of volume ~ 10 µl sitting on a planar surface is approximated as spherical-cap. For a constant volume droplet, *h* is droplet height, *R* is radius of curvature, θ is contact angle, *r* is base radius and Σ is surface area exposed to the ambient.

This approximation is valid for droplet diameter or length is below a length scale called as capillary length $\kappa^{-1}=\sqrt{\gamma/\rho g}$ where, γ is surface tension, ρ is the liquid density and g is acceleration due to gravity. For water λ = 2.7 mm. The elementary mathematics is used to derive relations between the contact angle θ and geometrical parameters like drop contact area *r*, radius of curvature *R*, exposed surface area Σ and drop height, Here volume (V_{cap}) of a droplet is kept fixed.

$$R=\left[\frac{3V_{cap}}{\pi(2-3\cos\theta+\cos^3\theta)}\right]^{1/3} \quad \ldots\ldots\ldots\ldots(12)$$

$$r=R\sin\theta=\left[\frac{3V_{cap}}{\pi(2-3\cos\theta+\cos^3\theta)}\right]^{1/3}\sin\theta \quad ..(13)$$

$$h=R\,(1-\cos\theta) \quad \ldots\ldots\ldots\ldots\ldots\ldots\ldots\ldots\ldots(14)$$

$$\Sigma=2\pi R\,h \quad \ldots\ldots\ldots\ldots\ldots\ldots\ldots\ldots\ldots\ldots\ldots(15)$$

The base area in contact with solid surface also given as $A_{base}=\pi r^2$. The drop of known volume on solid substrate can be deposited using micropipette. The volume is input parameter in this equation. Indeed the above common parameters are function of contact angle θ. In case

of the electrowetting this θ is function of the external voltage. Thus the above parameters of the spherical cap become function of the external voltage.

Experimental Techniques:

(i) Dielectric Coating for EW Application:

The materials for dielectric layer and bottom electrodes are not very specific in the EW applications. Any metallic surface covered with suitable hydrophobic film can be used to study EW phenomenon. Most of the EW studiers were done on Teflon (PTFE) film. It has low surface energy hence large CA of water. The commercially available films are in the range of tens of micrometer therefore high voltage is required to get the desired contact angle change. In several EW study at moderate voltages (< 100 V), thin coating from Teflon AF (DuPont USA)[16] or Cytop (Asahi Glass, Japan)[17] solution are commonly used. The coating from both these solution provides thickness in the range of nano-meter to micro-meter that depends mainly on the process parameters. Usually dip-coating and spin coating is used for this purpose. Brief procedure for Teflon AF dip-coating is described below. The Teflon AF dielectric layer can be dip-coated on any conductive surfaces. Here we used commercial Indium Tin Oxide (ITO) glass as an electrode. At the beginning, ITO glass was thoroughly cleaned successively in ultrasonic bath of diluted soap water, Acetone, isopropanal and ethanol. Finally it was dried in dry nitrogen jet. A dip coating machine is used for this dielectric coating. We used solution of amorphous fluropolymer Teflon AF1600 (DuPont, USA) in perfluorinated solvent FC40 (3M) at 6% w/v concentration. The ITO glass was slowly dipped at the speed of 15 cm/min and withdrawn after 10 sec. at same speed. These films were pre-dried in laminar flow and then in oven at 110 ^{o}C for 30 min. These films were cooled to room temperature and one more Teflon AF layer was applied using same experimental parameters. Finally substrates were heated at 160 °C for 10 minutes and 240 °C for 30 minutes in a vacuum oven for complete removal of solvent. The EW experiment also can be performed on several dielectric surfaces such as polystyrene[18], PVDF, SU8, PMMA, Parylene and multil lyares of SiO_x-SiN_x, Al_2O_3[10] and Ti_2O_5[19]covered with thin hydrophobic layer of either Teflon or Cytop etc.

Experiment Arrangement for Electrowetting:

The Electrowetting phenomenon can be conveniently studied using direct current (DC) as well as alternating current (AC) voltages. Electrowetting with DC voltages, one requires a variable DC power supply with the stable voltage magnitude from 0 to 200 V. The maximum voltage range can be decided from the dielectric thickness values. This voltage rating is sufficient for the dielectric layer of thickness 2-3 μm. For thick dielectric film like commercial Teflon tape, one needs a power supply rating of about 1 kV. These power ratings are same for AC voltage source. In case of AC voltage the frequency should be above 500 Hz and below 10 kHz. The lower cutoff frequency is limited by hydrodynamic response time, $\tau = l\frac{\mu}{\gamma}$, where l, is droplet diameter and μ is the liquid viscosity. The droplet diameter is mainly limited by the capillary length. The higher cut-off frequency is mainly decided by the droplet conductivity. At sufficient higher frequency, di-electrophoretic effects prevails therefore, EW which is derived from conductive droplet model, fails to predict the

change in CA with applied voltage magnitude at high frequency AC voltages.

Typical setups we used to prove the results are discussed here. A schematic of the experimental setup is shown in Fig. 7. It is consists of rectangular cuvette for placing a conductive substrate. A Function generator (HP 33120 A) was used as AC voltage source. Then this signal was amplified using custom built high voltage amplifier (Kemtec Engineering, Pune). The amplified voltage was given to water drop with bottom electrode at ground potential.

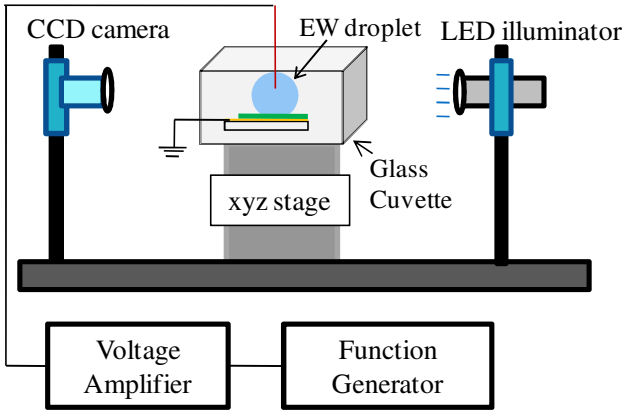

Fig. 7: Schematic of the experimental set up used for studying electrowetting on dielectric in oil ambient.

A CCD camera attached with the low magnification microscope was used for imaging the contact angle of the droplet at specified applied voltages. This drop was back illuminated using LED torch. All these were axially aligned and fixed on the stand as shown in figure. During experiment the cuvette table was kept horizontally flat using xyz position screws. The cuvette was filled with silicon oil. The level of the silicon oil was adjusted to keep the water drop submerged. Small amount of salt (1 mg /10 ml) was added in water to increase the conductivity. The salt does not change surface tension of water but increase the conductivity. Using micro pipette a water drop of 8 µl was dispensed on thin dielectric film. This is sessile drop arrangement as shown in Fig 7. After the nice optical arrangement, AC power supply was switch on and drop image was seen on computer screen. First contact angle was measured at 0 V. Then voltage was increased in steps of 4 V. For each AC voltage the corresponding droplet image was saved in the computer. The experiment was repeated many times and for increasing and decreasing voltage cycle. We used 1 kHz AC frequency in this study. The droplet image was analyzed using open source ImageJ 1.48 image processing software.

The results of the EW are discussed in following section.

Result and Discussion:

We have studied the electrowetting on dielectric by using wired geometry and interdigitated wire-free geometry and the response curves have been verified by plotting Young-Lippmann relation. Figure 8 shows the snapshot of EW water droplet in Silicone oil ambient and on wired electrowetting setup. It clearly shows decrease in CA with voltages.

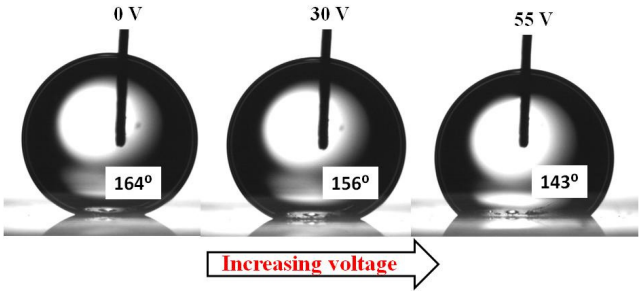

Fig. 8: Snapshots of EW on water droplet using wired setup for increasing voltage magnitude.

Also we have investigated electrowetting behavior for wire free geometry on interdigitated electrode. Figure 9 shows the snapshot of droplets illustrating contact angle variation with increasing

voltage for wire free geometry. Nature of response curves for wire free electrowetting geometry has close resemblance with wired geometry.

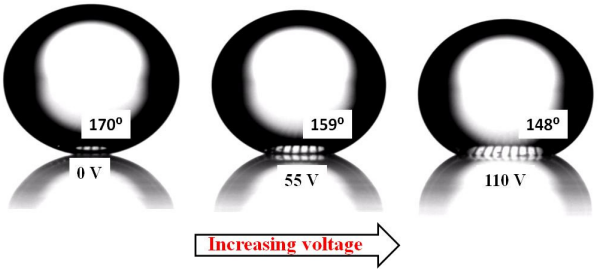

Fig. 9: Snapshot of electrowetted droplets with increasing voltage for wire free geometry.

The plot of the contact angle against applied voltage is shown in Fig. 10.

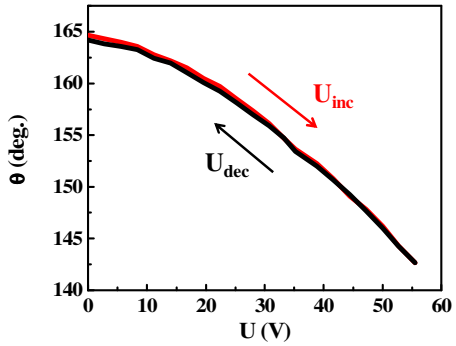

Fig. 10: Contact angle change with applied voltage for increasing and decreasing magnitude.

We then verify the electrowetting nature by plotting Young-Lippmann relation. The plot shown in Fig. 11 depicts cosine of the change in contact angle against voltage square. Indeed this shows linear variation. The change in contact angle with voltage shows excellent recovery. When voltage decreases to zero, the contact angle also attains the initial value.

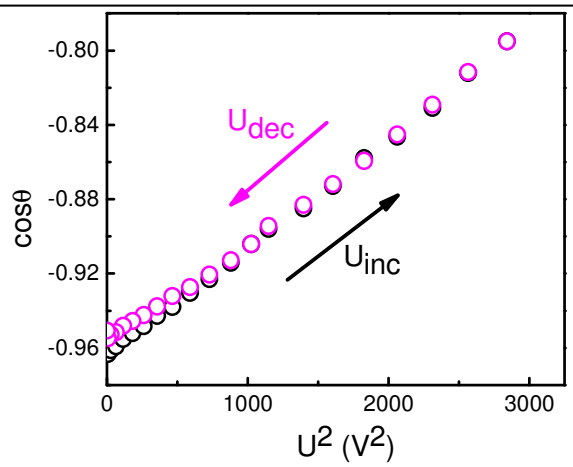

Fig. 11: Electrowetting on water drop: a contact angle change cos θ(U) against voltage square U^2 is plotted for $U = 0$ V to $U_{max} = 53.3$ V (rms). The increasing and decreasing voltage level are depicted as U_{inc} and U_{dec} respectively.

This plot can be used to obtain several physical parameters like interfacial tension of water-oil, dielectric constant and the thickness. From Young-Lippmann equation the slope of cos θ(U) versus U^2 curve has the value $\frac{\varepsilon\varepsilon_0}{2d\,\gamma_{LV}}$ where $\varepsilon\varepsilon_o$ is the permittivity of the dielectric medium, d is thickness and γ_{LV} is the interfacial tension of water with respect to the surrounding medium.

We measured thickness of Teflon film using profilometer and found to be 3.66 μm. The dielectric has to be as thin as possible but thin dielectric (~nm) often shows dielectric breakdown before achieving a desired change in contact angle. These values can be followed using EW slope value of the plot shown in Fig. 11. The slope of the graph between cos θ(U) and U^2 is found to be 5.671×10^{-5} SI unit. From the slope capacitance per unit area (C*) is calculated which is 4.514 μFm^{-2} which is constant for the given configuration of the dielectric medium. Contact angle hysteresis of around 3° can be seen during

reverse cycle. This is advantage of silicone oil ambient to the water droplet.

This plot can be employed to obtain a desired unknown value from constants. Recently such EW results are used for the estimation of interfacial tension of unknown liquids. We also determine the interfacial tension of water-silicone oil which is found to be 38 mNm^{-1} in excellent agreement with the reported value[11]. We now use the results of Electrowetting and the spherical cap model to demonstrate the variation in droplet geometry as a function of applied voltage.

Figure 12 shows plot of variation in base area of the droplet as a function of square of voltage.

Here we use the droplet images and estimated the base radius to find out the base area. Here it is called as experimentally determined base area (S_{exp}). The plot shows that base area linearly varies with square of applied voltage U.

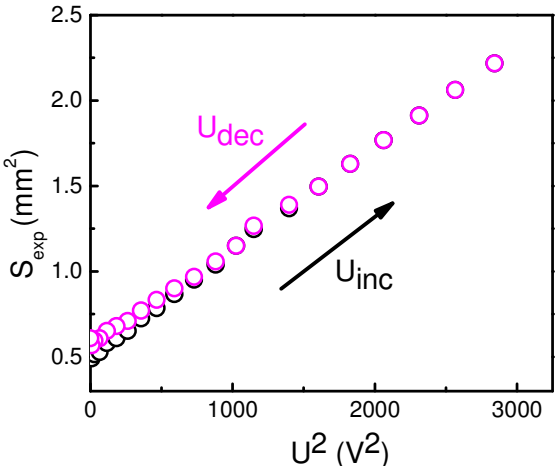

Fig. 12: The base area of the droplet determined experimentally is plotted against voltage square.

We also calculated the base area of the droplet from base radius related to contact angle as given in the Eq. 13. The EW contact angles corresponding to all the voltage values are used to determine the value of the base area. This base area is termed as theoretical base area S_{the} plotted as voltage square in Fig. 13.

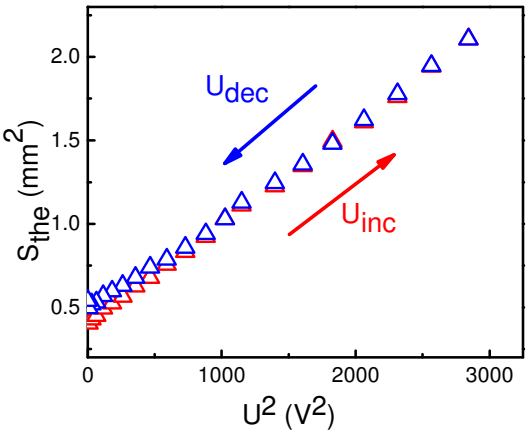

Fig. 13: Plot shows a base area of droplet calculated from closed form of spherical cap plotted against U^2. The graph is again linear with voltage square.

Here the plot shows linear variation with voltage square. We compare our experimental results with the value estimated from spherical cap model in Fig. 14.

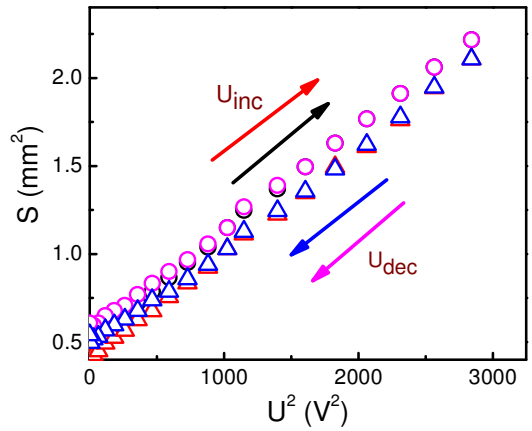

Fig. 14: Comparison between experimentally determined base area and theoretically calculated base area for given variation in potential. Both are closely overlapping with each other.

Experimentally measured and theoretically calculated base area both are matching fairly well. This linear nature helps in tuning of base area of the droplet with respect to applied voltage. In the working regime of contact angle θ, varying from 164° to 143°, is almost linear with U^2. The small

deviation in the experimental and theoretical value is mainly due to the error in volume measured by the optical techniques and actual volume of the droplet taken from micro-pipette.

Figure 15 shows variation in capacitance of the system as a function of applied voltage square

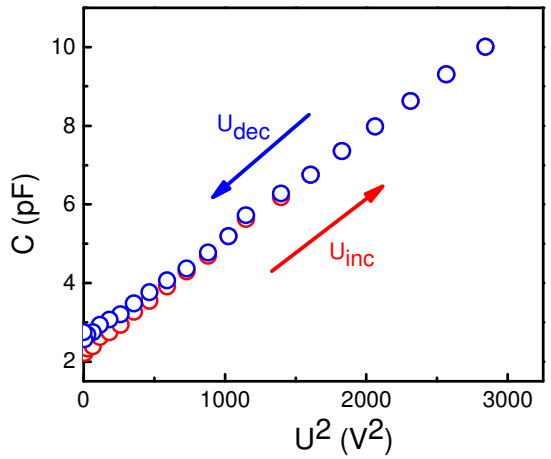

Fig. 15: The capacitance of the system plotted against square of applied voltage.

The capacitance of the system shows fairly linear variation with the voltage square. In EW based technique capacitance of the system is varied by external voltage and not by any mechanical movement. This is implemented in several electronic- frequency tuning devices.

The liquid droplet forming a nice spherical cap is known for its optical properties like lens. A droplet sitting on leaves acts as lens. EW provides continuous change in contact angle with external voltage. The leasing property of such droplet depends on the radius of curvature. Therefore we plot radius of curvature of EW droplet as a function of voltage square as show in Fig. 16.

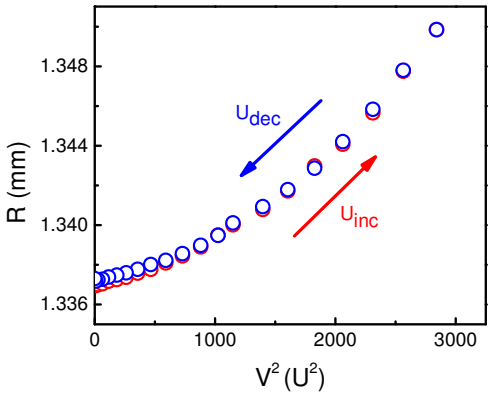

Fig. 16: Plot of Radius of curvature *R* versus voltage square.

The dependency of *R* on contact angle θ, and hence on *U* is quite complex. Dependency can be seen from Eq .12 However, voltage dependent changes in the radius of curvature are possible through EW. This does not require any mechanical input.

The droplet height variation can be used for EW based actuation. Figure 17 shows variation in the droplet height as a function of voltage square.

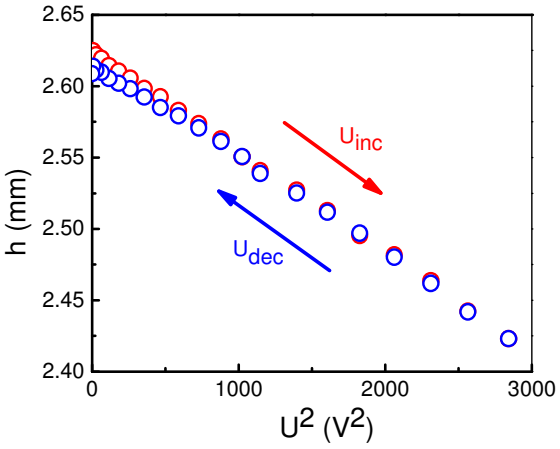

Fig. 17: Behavior of height of the drop on voltage square.

This shows that droplet height *h* decreases linearly with voltage square. Typically the mechanical

actuation in micrometer range can be easily achieved using EW.

The surface area in contact with ambient (here silicone oil) is estimated from Eq. 15 and plotted in Fig. 18.

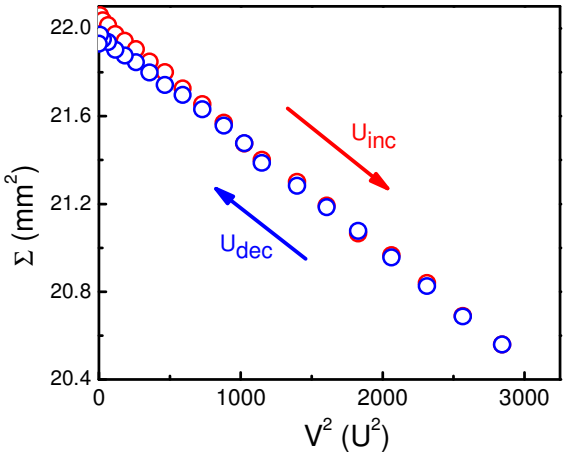

Fig. 18: Surface area of spherical droplet in contact to Silicone oil is plotted against voltage square.

The plot shows linear variation in the surface area with the voltage square.

We demonstrated that various geometrical parameter of electrowetted spherical cap can be varied by external voltage. This is non-contact method also reversible and high reproducibility. The oil ambient arrest evaporations thus it has high self-life. More applications of EW are discussed in the tutorial review by Shamai *et al*[20].

In the development of commercial applications especially the liquid lens, Bruno Berge[8] has developed for the first time and set up a production unit named "Varioptics" in Lyon, France[21]. During the same time EW has been used for video speed display. A Dutch company "Liquivista" founded in 2006 at Eindhoven as a spin-off from Philips has developed colour e-paper video screens that can work in the presence and absence of backlight[22]. More recently, Mishra *et al* demonstrated ideal aspherical lens by applying electric field to a drop entrapped in an aperture controlled hydrostatically[23]. Herein, liquid-liquid meniscus shape is altered by simultaneously altering the electrostatic force and Laplace pressure. In this lens system, along with alteration of focal length, longitudinal spherical aberration (LSA) value can be altered achieving enhanced optical performance.

The EW based high speed actuation of micro-lens array has been recently demonstrated. The focal length of all 100 micro-lens array has been simultaneously modulated at frequency beyond 1 kHz[24]. In case of the micro-fluidics lab-on-chip systems, electrowetting principle is used to create electrostatic potential well for the droplet sorting and manipulation of droplet in a desired micro-channel[25]. The EW principle is also used in the fundamental studies that involve controlled wetting transition from superhydrophobic Cassie-Baxter state to Wenzel state on pillar-structured surface[26]. Recently a wire-free electrowetting also called as dielectrowetting is used for the high resolution and high speed optical shutters which can be used as large area optical shutters in household window applications[27].

Many new application based on the EW as well as dielectrowetting principle can be envisaged in the future. However, there are some limitations in EW phenomenon[28]. The basic limitation is as follows: Theoretically, Young-Lippmann equation states that CA decreases to any amount (complete wetting) with external applied voltage. In practical situation, one can decrease CA to a curtain level well above the complete wetting state and reaches to saturation state. Figure 18 shows the CA saturation behavior in the EW. In the saturation regime, applied voltage does not cause any change in CA deviating from Young-Lippmann eq.

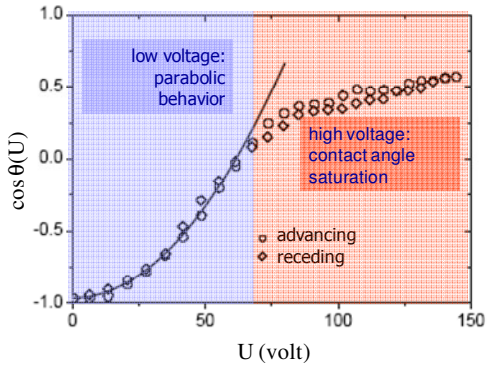

Fig. 18: CA variation cos θ (*U*) plotted as applied voltage *U*.

Several theories are proposed to explain the CA saturation such as ionization of air at three phase contact line, charge trapping, dielectric leakage[29-31], defect in dielectric and dielectric breakdown. However consensus amongst the theories has not been reached yet. Therefore EW and dielectrowetting principle is being continuously used in the Young-Lippmann regime for increasing number of applications discussed in this article.

Conclusions:

In conclusion, we presented a short review on the wetting of liquid on planar surface. Wetting of liquid on solid surface is described by Young-Dupre' equation. The electrowetting on dielectric (EW) is described in detail using two basic approaches. In case of EW, the CA of liquid can be conveniently and reversibly changed just by external voltage. EW is noncontact and fast process and operates on simple capacitive design. Therefore it is used in many applications in optics and display devices. Also force imparted by the electric field on the droplet is used for transport, actuation, splitting, merging and mixing of the tiny amount of liquid inside micro-fluidic channel. It is also used in the physical characterization of the liquid including interfacial tension and rheology.

Acknowledgment: One of the authors AGB would like to acknowledge BCUD, SPPU for research funding. Also YBS, would like to acknowledge UCG for fellowship.

References:

1. T. Young, Philos. Trans. Roy Soc. London 95, 65 (1805).
2. P.G. de Gennes, F. Brochard-Wyart, and and D. Quere, Capillary and Wetting Phenomenon: Drops, Bubbles, Pearls, Springer: New York (2004).
3. G. Karapetsas, K. C. Sahu, K. Sefiane and O. K. Matar, Langmuir 30 (15), 4310-4321 (2014).
4. B. Yan, J. G. Tao, C. Pang, Z. Zheng, Z. X. Shen, C. H. A. Huan and T. Yu, Langmuir 24 (19), 10569-10571 (2008).
5. F. Mugele and J. C. Baret, J Phys-Condens Mat 17 (28), R705-R774 (2005).
6. G. Lippmann, Ann. Chim. Phys. 5, 495 (1875).
7. M. Vallet, B. Berge and L. Vovelle, Polymer 37 (12), 2465-2470 (1996).
8. B. Berge and J. Peseux, Eur Phys J E 3 (2), 159-163 (2000).
9. R. A. Hayes and B. J. Feenstra, Nature 425 (6956), 383-385 (2003).
10. J. Heikenfeld and A. J. Steckl, Appl Phys Lett 86 (15) (2005).
11. A. G. Banpurkar, K. P. Nichols and F. Mugele, Langmuir 24 (19), 10549-10551 (2008).
12. A. G. Banpurkar, M. H. G. Duits, D. van den Ende and F. Mugele, Langmuir 25 (2), 1245-1252 (2009).

13. R. B. Fair, Microfluid Nanofluid 3 (3), 245-281 (2007).
14. L. D. Landau and E. M. Lifshitz, Pergamon Press LTD. Vol. 8 (1963).
15. H. J. J. Verheijen and M. W. J. Prins, Langmuir 15 (20), 6616-6620 (1999).
16. E. Seyrat and R. A. Hayes, J Appl Phys 90 (3), 1383-1386 (2001).
17. N. B. Crane, A. A. Volinsky, P. Mishra, A. Rajgadkar and M. Khodayari, Appl Phys Lett 96 (10) (2010).
18. B. Bhushan and Y. L. Pan, Langmuir 27 (15), 9425-9429 (2011).
19. Y. Y. Lin, R. D. Evans, E. Welch, B. N. Hsu, A. C. Madison and R. B. Fair, Sensor Actuat B-Chem 150 (1), 465-470 (2010).
20. R. Shamai, D. Andelman, B. Berge and R. Hayes, Soft Matter 4 (1), 38-45 (2008).
21. http://www.varioptic.com/.
22. http://www.liquavista.com/.
23. K. Mishra, C. Murade, B. Carreel, I. Roghair, J. M. Oh, G. Manukyan, D. van den Ende and F. Mugele, Sci Rep-Uk 4 (2014).
24. C. U. Murade, D. van der Ende and F. Mugele, Opt Express 20 (16), 18180-18187 (2012).
25. R. de Ruiter, A. M. Pit, V. M. de Oliveira, M. H. G. Duits, D. van den Ende and F. Mugele, Lab Chip 14 (5), 883-891 (2014).
26. G. Manukyan, J. M. Oh, D. van den Ende, R. G. H. Lammertink and F. Mugele, Phys Rev Lett 106 (1) (2011).
27. A. Russell, E. Kreit and J. Heikenfeld, Langmuir 30 (18), 5357-5362 (2014).
28. F. Mugele, Soft Matter 5 (18), 3377-3384 (2009).
29. A. Quinn, R. Sedev and J. Ralston, J Phys Chem B 109 (13), 6268-6275 (2005).
30. A. G. Papathanasiou and A. G. Boudouvis, Appl Phys Lett 86 (16) (2005).
31. A. G. Papathanasiou, A. T. Papaioannou and A. G. Boudouvis, J Appl Phys 103 (3) (2008).